Growth and single-crystal refinement of phase-III potassium nitrate, KNO_3

Evelyn J. Freney,[a]***** **Laurence A. J. Garvie,**[a] **Thomas L. Groy**[b] **and Peter R. Buseck**[a,b]

[a]School of Earth and Space Exploration, Arizona State University, Tempe, Arizona 85287-1404, USA, and [b]Department of Chemistry and Biochemistry, Arizona State University, Tempe, Arizona 85287-1604, USA

Correspondence e-mail: efreney@asu.edu

Oriented single crystals of the high-temperature phase of KNO_3 (phase III), a ferroelectric compound that may also occur as an atmospheric aerosol particle, were grown at room temperature and pressure by atomizing a solution of KNO_3 in water and allowing droplets to dry on a glass substrate. The crystals are up to 1 mm across and are stable unless mechanically disturbed. There is no evidence of the spontaneous transformation of phase III to the room-temperature stable phase (phase II), even after several months. Single-crystal structure determinations of phase III were obtained at 295 and 123 K. The unit cell regained its room-temperature dimensions after warming from 123 K. The phase-III KNO_3 structure can be viewed as the stacking parallel to the c axis of alternating K atoms and planar NO_3 groups. The NO_3 groups connect the planes of K atoms, where each O is fourfold coordinated to one N and three K. Each K atom has nine O nearest neighbors, with three bonds at 2.813 and six at 2.9092 Å. The interatomic K—N—K distance alternates from 5.051 to 3.941 along the c axis. The N—O distances increase from 1.245 (2) Å at 295 K to 1.2533 (15) Å at 123 K. The nitrate group has a slight non-planarity, with the N atoms 0.011 Å above the O plane and directed toward the more distant K of the K—N—K chain.

1. Introduction

Nitrates such as KNO_3, $Ca(NO_3)_2$, $NaNO_3$ and NH_4NO_3 are constituents of the tropospheric aerosol and are typical of particles that have undergone reactions with gaseous nitric acid. KNO_3 is common in aerosols derived from biomass burning (Li *et al.*, 2003) and blowing dust (Ro *et al.*, 2005). It is important to know the form of KNO_3 or other nitrates in the atmosphere as different phases can exhibit different physical and chemical properties (Wu & Chan, 2008). KNO_3 is also an important ingredient in explosives and propellants (Engelen *et al.*, 2002) and shows promise as a material for random access memory (RAM) devices (Kumar & Nath, 2003). In addition, one of the polymorphs of KNO_3, phase III, exhibits ferroelectric properties (Chen & Chernow, 1967). Given all this interest, there has been considerable study into the physical, structural and chemical properties of KNO_3.

Seven polymorphs of KNO_3 are known, three of which are stable at ambient pressure (Nimmo & Lucas, 1976; Rapoport & Kennedy, 1965; Scott *et al.*, 1987). Room-temperature KNO_3 (phase II) is orthorhombic (*Pnma*) and has the

doi:10.1107/S0108768109041019

Table 1
Crystal data and results of structure refinement of phase-III KNO_3 at 295 and 123 K.

For all structures: KNO_3, M_r = 101.11, hexagonal, $R3m$, Z = 3. Experiments were carried out with Mo $K\alpha$ radiation using a Bruker SMART APEX diffractometer. Data collection used ω scans. Absorption was corrected for by multi-scan methods, *SADABS*, Version 2.10 (Bruker, 2003). Refinement was with 0 restraints. The absolute structure was obtained using Flack (1983).

	Room temperature	123 K
Crystal data		
a, c (Å)	5.4698 (8), 8.992 (3)	5.4325 (2), 8.8255 (7)
V (Å^3)	232.99 (8)	225.56 (2)
μ (mm^{-1})	1.50	1.55
Crystal size (mm)	0.11 × 0.08 × 0.02	0.11 × 0.08 × 0.02
Data collection		
Monochromator	Graphite	Graphite
T_{min}, T_{max}	0.858, 0.966	0.854, 0.965
No. of measured, independent and observed [$I > 2\sigma(I)$] reflections	764, 157, 157	755, 155, 155
R_{int}	0.0000	0.0000
Range of h, k, l	$h = -6 \to 0$, $k = 0 \to 7$, $l = -11 \to 11$	$h = -6 \to 0$, $k = 0 \to 7$, $l = -11 \to 11$
Refinement		
$R[F^2 > 2\sigma(F^2)]$, $wR(F^2)$, S	0.022, 0.054, 1.23	0.017, 0.041, 1.14
No. of reflections	157	155
No. of parameters	13	12
$\Delta\rho_{max}$, $\Delta\rho_{min}$ (e Å^{-3})	0.13, −0.16	0.18, −0.19
Flack parameter	−0.03 (8)	−0.05 (7)

Computer programs: *SMART*, *SAINT*, *SHELXTL* (Bruker, 2003), *SHELXS*97, *SHELXL*97 (Sheldrick, 2008).

aragonite structure (Sawada *et al.*, 1958). When phase II is heated above 401 K it transforms to the trigonal form ($R\bar{3}m$), which possesses the calcite structure (phase I; Nimmo & Lucas, 1976). Another polymorph (phase III) forms upon cooling phase I below 401 ± 20 K (Sawada *et al.*, 1958) and is metastable at lower temperatures (Kennedy, 1972). Phase III has received considerable attention because of its ferroelectric properties (Nimmo & Lucas, 1976; Poprawski *et al.*, 2007; Rapoport & Kennedy, 1965). The structure and stability of the KNO_3 polymorphs have been studied using *ab initio*, electrochemical and crystallographic methods (Smith & Clarke, 1989; Sawada *et al.*, 1958; Nimmo & Lucas, 1976; Christensen *et al.*, 1996).
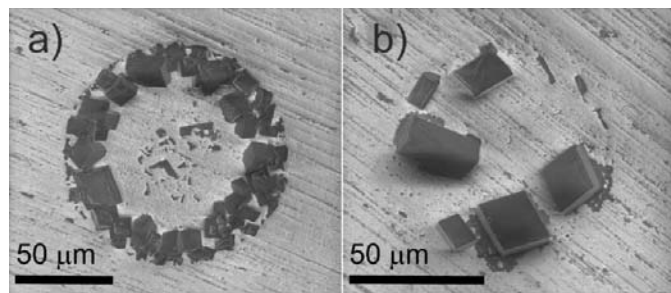

Figure 1
SEM images of atomized and dried KNO_3 particles on a glass slide. (*a*) Crystals grown from a deposited drop of KNO_3. (*b*) Higher magnification image of rhomboid-shaped crystals.

Although phase III is reportedly metastable at room temperature and pressure (Rapoport & Kennedy, 1965), it has been formed at ambient conditions. For example, Kennedy (1972) grew phase III on glass slides by allowing a droplet of KNO_3 solution to dry at room temperature. These crystals persisted for 2 months in a desiccator, but when mechanically disturbed they transformed to phase II. Phase III was also shown to form when phase I was cooled from 401 K to room temperature if the preheating temperatures and cooling rates were controlled (Murugan *et al.*, 1999). Thin films of phase III produced by vapor-transport deposition at room temperature (Nolta & Schubring, 1962) can persist for many years in suitably thin films (Aydinol *et al.*, 2007). Other studies have shown that the introduction of an ammonium ion can stabilize KNO_3 phase III at room temperature (Holden & Dickinson, 1975). Despite all this work, no single-crystal structure determinations have been obtained.

Here we describe a novel method for the room-temperature growth of single crystals of phase-III KNO_3 and refine its structure at both room temperature and 123 K.

2. Experimental

A 1 *M* solution (18.3 *M* nanopure water) of KNO_3 (Aldrich 99.99%) was atomized using a constant-output atomizer (TSI 3076) with dry N_2 (35 p.s.i.) as the carrier. The atomized droplets were deposited onto glass or single-crystal quartz slides, with and without grease coating. Powder X-ray diffraction (XRD) patterns were acquired with a Rigaku powder X-ray diffractometer employing Cu $K\alpha$ radiation and operating at 50 kV and 30 mA.

Single-crystal data were acquired with a Bruker Smart APEX CCD area detector employing Mo $K\alpha$ radiation. The data were integrated and reduced using *SAINT* (Bruker, 2003) from the Bruker suite of software. Absorption corrections were performed using the *SADABS* (Bruker, 2003) program. The Bruker *SHELXTL* (Bruker, 2003) software package was utilized to solve the structures by direct methods. The refinements were performed against all F^2 with anisotropic displacement parameters. Single-crystal data for phase-III KNO_3 were measured at room temperature (295 K) and at 123 K (Tables 1–4).[1] The structure data were reacquired after

---

[1] Supplementary data for this paper are available from the IUCr electronic archives (Reference: BP5023). Services for accessing these data are described at the back of the journal.

Table 2
Bond lengths (Å).

Atom 1	Atom 2	Distance (295 K)	Distance (123 K)
K1	O1	2.813 (2)	2.7799 (14)
K1	O1	2.814 (2)	2.8778 (5)
K1	N1	3.2962 (11)	3.2643 (9)
N1	O1	1.245 (2)	1.2533 (15)
O1	K1	2.9092 (8)	2.7798 (14)

Table 3
Comparison of lattice dimensions for phase-III KNO_3 at 364 (Nimmo & Lucas, 1976), 295 and 123 K.

Phase	a	c
III (364 K)	5.487	9.156
III (295 K)	5.4698	8.992
III (123 K)	5.4325	8.8255

Table 4
Comparison of bond angles (°) and bond lengths (Å) phase-III KNO_3 at 364 (Nimmo & Lucas, 1976), 295 and 123 K.

	Nimmo & Lucas (1976), 364 K	This work, 295 K	This work, 123 K
K—O	2.870	2.813	2.780
N—O	1.273	1.245	1.253
K—N	5.448	5.051	4.979
N—K	3.708	3.941	3.846
O—N—O	115.769	119.956	119.984

the crystal was warmed back to room temperature. The structure did not show any discernable changes after warming so only the 295 and 123 K data are listed. Bond angles and selected bond distances are shown in Table 4.

Crystals were imaged with a NOVA 200 Nanolab Dual-Beam FIB scanning electron microscope (SEM) at 0.5 and 1 kV (Fig. 1). Samples were imaged without coating. Optical images were acquired on a light microscope using both plane and polarized light (Fig. 2).

3. Results and discussion

3.1. Crystal growth

The atomizer used in this study (TSI model 3076) produces of the order of 10^8 particles s^{-1}, with diameters ranging from 0.5 to 5 μm. A wet aerosol from the atomizer was directed onto the slides and dried in air, producing a white film consisting of euhedral crystals (Figs. 1 and 2). Growth of crystals larger than ca >50 μm occurred at relative humidities (RH) greater than 20%. When the RH dropped below 20%, only crystals ca 10 μm or smaller grew. Crystals to 1 mm were grown and it is thought that several aerosol droplets coalesced to form larger droplets, which subsequently dried to form single crystals.

Powder XRD patterns of these films show reflections at 3.268 and 3.004 Å only (Fig. 3a), indicating that crystals grown on the glass slide are well oriented. These peaks are close to the 012 and 003 reflections of phase III (PDF 01-070-0205; Nimmo & Lucas, 1976). When the film was scraped and repositioned on the slide, the XRD pattern lacked the peaks at 3.268 and 3.004 Å, but instead matched those of phase-II KNO_3 (Fig. 3b).

Examination of the slide with an optical microscope showed bladed, threefold twinned and rhomboid-shaped crystals (Fig. 2a). Yanagi (1965) also observed this mixture of shapes and reported that it depended on the cooling rate of saturated solutions. With polarized light, the bladed crystals are isotropic, consistent with their optic axis oriented parallel to the incident light (and hence perpendicular to the plane of the glass slide). It is these isotropic crystals that give rise to the 003 reflection on the XRD pattern (Fig. 2b). The rhombohedral
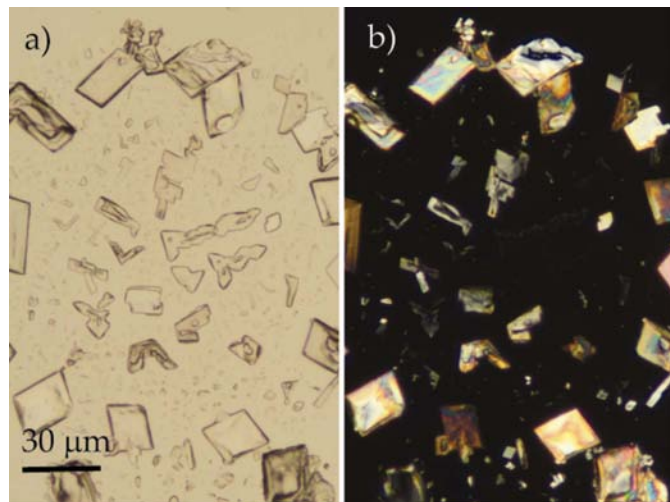

Figure 2
Optical images of crystals on a glass substrate viewed with (a) unpolarized light and (b) polarized light. The bladed crystals occur primarily near the center of the image with larger rhombohedral-shaped crystal surrounding.
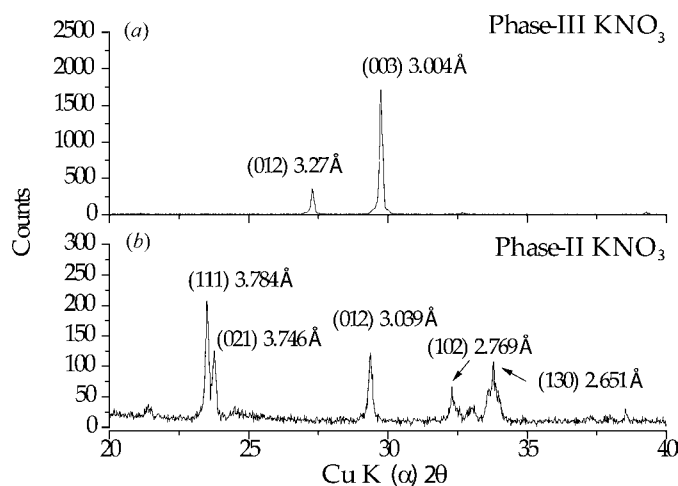

Figure 3
(a) Powder XRD pattern of phase-III KNO_3. (b) XRD pattern of the material in (a) after it has been scraped off the slide and redeposited. The XRD pattern corresponds to that of phase-II KNO_3.
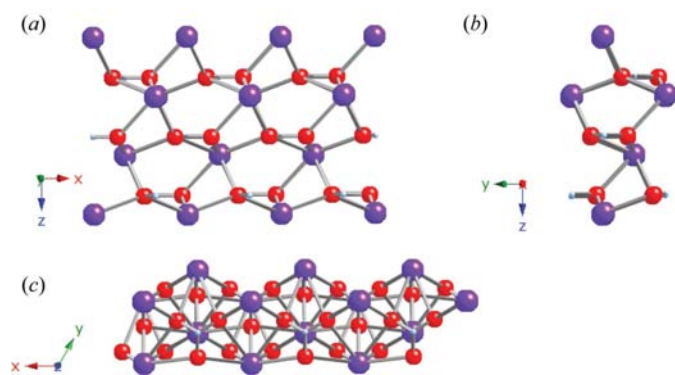
Figure 4
Images of the KNO₃ crystal structure (a) viewed parallel to the b-axis showing that the structure consists of alternating layers of K and NO₃ along z, (b) viewed parallel to the a-axis and (c) viewed parallel to the c-axis.
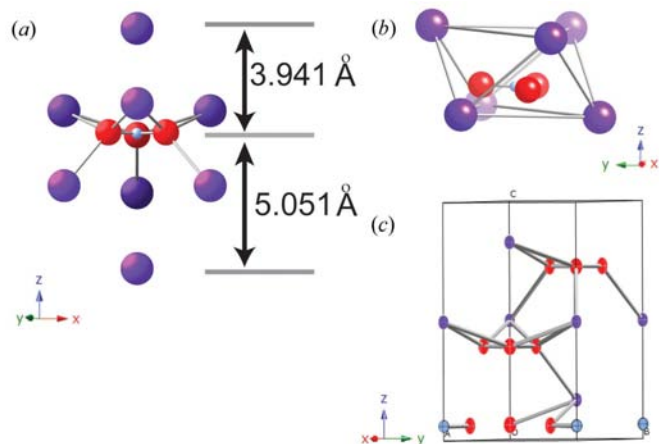

Figure 5
Images of the KNO₃ crystal structure viewed as (a) eight K atoms around a NO₃ group and illustrating the variable K—N—K distances. (b) A polyhedral unit defined by the K at the vertices and NO₃ below the polyhedral centroid. (c) Basic structure cell with displacement ellipsoids. The unit cell is indicated by dotted lines.
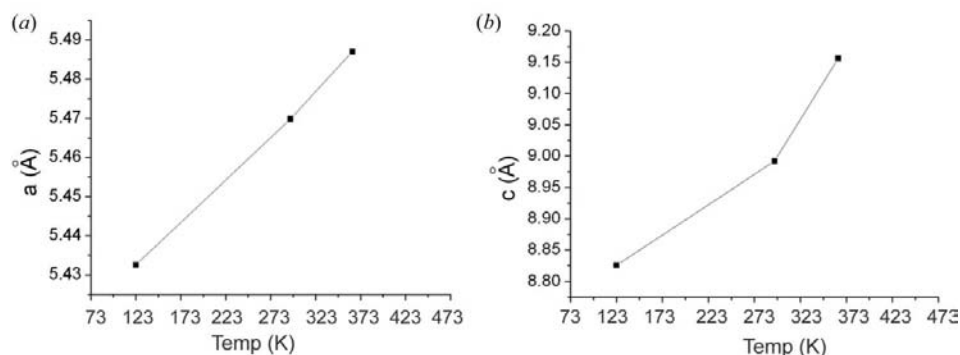

Figure 6
Variation of (a) the a-axis and (b) the c-axis as a function of temperature. The data point at 364 K is from Nimmo & Lucas (1976).

crystals are optically anisotropic and give rise to the 012 reflection in the powder XRD patterns. Attempts to dislodge the crystals from the glass slide caused a wave of birefringence to move through the crystals, corresponding to the change from phase III to II. Any mechanical disturbances, even those from the edges of cooling crystals, are sufficient to propagate the phase III to phase II transition. For this reason, it is possible that phase-III KNO₃ does not normally form when bulk phase I is cooled below its stability region.

Atomization of the KNO₃ solution onto grease-covered slides produced crystals of similar shape and size as on grease-free glass slides. Powder XRD patterns of these slides show only the 012 and 003 peaks of phase-III KNO₃. These crystals could be moved in the grease and removed from the slide without changing to phase-II KNO₃.

3.2. Structure description of phase-III KNO₃

Single-crystal X-ray diffraction of a crystal deposited onto the grease refines with a hexagonal unit cell, space group $R3m$, and cell dimensions $a = b = 5.4698 (8)$ and $c = 8.992 (3)$ Å (Table 1). The phase-III KNO₃ structure can be viewed as the stacking of alternating planes of K atoms and NO₃ groups parallel to the c-axis (Fig. 4a). The NO₃ groups connect the planes of K atoms, where each O is fourfold coordinated to one N and three K (Fig. 5a). Each K atom has nine O nearest neighbors, with three bonds at 2.813 (2) Å and six at 2.9092 (8) Å. There is a small but measurable non-planarity of the NO₃ groups, with the N atoms 0.011 Å above the O plane and directed towards the more distant K of the K—N—K chain.

The basic building block of the structure can be visualized as a chair-like unit with a NO₃ group at the center and three K atoms above and below (Fig. 5a). The three K atoms above the NO₃ groups are rotated 60° with respect to the three below (Figs. 5a and b). The O—K distances are 2.9092 (8) Å for the O below the NO₃ group and 2.813 (2) Å above. The N of the NO₃ groups is offset along the c axis, with repeat K—N distances of 3.941 and 5.051 Å (Fig. 5a). The ferroelectricity likely arises from the NO₃ group existing slightly off-center along the c axis of the unit cell (Elkabbany et al., 1995), a result reached from the X-ray powder diffraction data of Nimmo & Lucas (1973). Furthermore, the NO₃ group can jump between these two equivalent positions (K—N 3.941 or 5.051 Å) following the reversal of the external electric field (Sawada et al., 1961).

At 123 K the cell dimensions shorten to $a = b = 5.4325 (2)$ and $c = 8.8255 (7)$ Å (Table 1), a decrease of 1.85% along c and 0.68% along a (Table 3 and Fig. 6). The unit-cell dimensions of the cooled crystal return to their original values on warming to room temperature. The

structure at low temperatures is identical to that at room temperature, but with small changes in the bond lengths (Table 4). The K—O bond distances decrease upon cooling, whereas the N—O lengths increase from 1.245 to 1.2533 Å. Nimmo & Lucas (1973) also observed an increase in the N—O bond lengths for phase II KNO_3 when the temperature was changed from 373 to 298 K.

Our room- and low-temperature c-axis dimensions are significantly shorter than measured at higher temperatures, e.g. 9.11 Å at 393 K (Stromme, 1969), 9.163 Å at 391 K (Christensen et al., 1996), and 9.156 at 364 K (Nimmo & Lucas, 1976). A decrease occurs from 9.163 to 9.002 Å as phase-III KNO_3 is cooled from 383 to 303 K (Christensen et al., 1996). Our room-temperature (295 K) c-axis value of 8.992 (3) Å is close to the value of 9.002 Å measured at 303 K by Smith & Clarke (1989). This shift in the c-axis dimension is responsible for the small differences of the 012 and 003 reflections in our powder XRD patterns (Fig. 3a) compared with the data reported in PDF 01-070-0205. This unusual thermal expansion of the c-axis appears to be closely connected to the rotations of the nitrate ions, which are thought to be responsible for initiating the phase II to I and phase I to III transitions (Lu & Hardy, 1990, 1991). We observed that if a single-crystal of phase-III KNO_3 is disturbed, it transforms to polycrystalline phase-II KNO_3.

4. Conclusion

Atomization is commonly used to produce aerosols for the laboratory study of atmospheric particles. For some materials, such as KNO_3, this method of sample preparation may result in polymorphs with properties different than those expected. Additionally, the phases of KNO_3 and other nitrates in the atmosphere are not well defined but, as this work shows, could easily form when solution droplets dry on a substrate. It remains to be determined whether phase-III KNO_3 occurs in atmospheric aerosols.

We grew single crystals of phase-III KNO_3 up to 1 mm across under room temperature and pressure by atomizing aqueous solutions of KNO_3 and depositing the droplets onto a grease-coated substrate. To our knowledge, we determined the first single-crystal structure of phase-III KNO_3, producing results that can be used in studies on its ferroelectric properties. Furthermore, these crystals can be moved and picked up as well as exposed to temperatures varying from 295 to 123 K without undergoing a relaxation of the structure to the non-ferroelectric phase II.

References

Aydinol, M. K., Mantese, J. V. & Alpay, S. P. (2007). *J. Phys. Condens. Matter*, **19**, 496210.

Bruker (2003). *SADABS, SAINT, SHELXTL* and *SMART*. Bruker AXS Inc., Madison, Wisconsin, USA.

Chen, A. & Chernow, F. (1967). *Phys. Rev.* **154**, 493–505.

Christensen, A., Norby, P., Hanson, J. C. & Shimada, S. (1996). *J. Appl. Cryst.* **29**, 265–269.

Elkabbany, F., Abdelkader, M. M., Tosson, M. & Elkhwass, E. (1995). *Thermochim. Acta*, **256**, 281–289.

Engelen, K., Lefebvre, M. H. & Hubin, A. (2002). *Propellants Explos. Pyrotech.* **27**, 290–299.

Flack, H. D. (1983). *Acta Cryst.* A**39**, 876–881.

Holden, J. R. & Dickinson, C. W. (1975). *J. Phys. Chem.* **79**, 249–256.

Kennedy, S. W. (1972). *J. Cryst. Growth*, **16**, 274–276.

Kumar, N. & Nath, R. (2003). *J. Phys. D Appl. Phys.* **36**, 1308–1313.

Li, J., Posfai, M., Hobbs, P. V. & Buseck, P. R. (2003). *J. Geophys. Res.* **108**, 8484–8495.

Lu, H. M. & Hardy, J. R. (1990). *Ferroelectrics*, **111**, 43–47.

Lu, H. M. & Hardy, J. R. (1991). *Phys. Rev. B*, **44**, 7215–7224.

Murugan, R., Ghule, A. & Chang, H. (1999). *J. Appl. Phys.* **86**, 6779–6788.

Nimmo, J. K. & Lucas, B. W. (1973). *J. Phys. Solid State Phys.* **6**, 201–211.

Nimmo, J. K. & Lucas, B. W. (1976). *Acta Cryst.* B**32**, 1968–1971.

Nolta, J. P. & Schubring, N. W. (1962). *Phys. Rev. Lett.* **9**, 285–286.

Poprawski, R., Rysiakiewicz-Pasek, E., Sieradzki, A., Man, A. & Polanska, J. (2007). *J. Non-Cryst. Solids*, **353**, 4457–4461.

Rapoport, E. & Kennedy, G. C. (1965). *J. Phys. Chem. Solids*, **26**, 1995–1997.

Ro, C. U., Hwang, H., Chun, Y. & Van Grieken, R. (2005). *Environ. Sci. Technol.* **39**, 1409–1419.

Sawada, S., Asao, Y. & Nomura, S. (1961). *J. Phys. Soc. Jpn*, **16**, 2486.

Sawada, S., Nomura, S. & Fujii, S. (1958). *J. Phys. Soc. Jpn*, **13**, 1549.

Scott, J. F., Zhang, M. S., Godfrey, R. B., Araujo, C. & Mcmillan, L. (1987). *Phys. Rev. B*, **35**, 4044–4051.

Sheldrick, G. M. (2008). *Acta Cryst.* A**64**, 112–122.

Smith, W. & Clarke, J. H. R. (1989). *J. Chem. Phys.* **90**, 6610–6618.

Stromme, K. O. (1969). *Acta Chem. Scand.* **23**, 1625.

Wu, H. B. & Chan, C. K. (2008). *Atmos. Environ.* **42**, 313–322.

Yanagi, T. (1965). *J. Phys. Soc. Jpn*, **20**, 1351–1365.